Journal of Biomechanics 117 (2021) 110245

Contents lists available at ScienceDirect

Journal of Biomechanics

journal homepage: www.elsevier.com/locate/jbiomech
www.JBiomech.com

Large magnitude of force leads to NO-mediated cell shrinkage in single osteocytes implying an initial apoptotic response

Nobuhiko Nakao [a,b], Izumi Mori [a,b], Junko Sunaga [b], Taiji Adachi [a,b,c,*]

[a] Department of Micro Engineering, Graduate School of Engineering, Kyoto University, 53 Shogoin-Kawahara-cho, Sakyo, Kyoto 606-8507, Japan
[b] Institute for Frontier Life and Medical Sciences, Kyoto University, 53 Shogoin-Kawahara-cho, Sakyo, Kyoto 606-8507, Japan
[c] Department of Mammalian Regulatory Network, Graduate School of Biostudies, Kyoto University, 53 Shogoin-Kawahara-cho, Sakyo, Kyoto 606-8507, Japan

ARTICLE INFO

Article history:
Accepted 3 January 2021

Keywords:
Osteocyte
Mechanical stimulus
Apoptosis
Nitric oxide
Magnetic tweezer

ABSTRACT

Damage accumulation in the bone under continuous daily loading causes local mechanical overloading known to induce osteocyte apoptosis, which promotes bone resorption to repair bone damage. However, only a few studies have investigated the mechanism of apoptosis in mechanically overloaded osteocytes. As mechanically stimulated osteocytes produce nitric oxide (NO), which triggers apoptosis in various cell types, we aimed to elucidate the mechanism underlying apoptosis in mechanically overloaded osteocytes, focusing on intracellular NO. To investigate the effects of force magnitude on apoptosis and intracellular NO production, we isolated osteocytes from DMP1-EGFP mice and subjected them to quantitative local forces via fibronectin-coated micro beads targeting integrin on the cell surface using a magnetic tweezer. Cell shrinkage was microscopically examined, and intracellular NO production was visualized using DAR-4 M. Mechanical stimulation revealed relationships between force magnitude, apoptosis, and intracellular NO production. The application of a smaller force resulted in no significant cell shrinkage or intracellular NO production; however, a larger force caused a rapid increase in intracellular NO production followed by cell shrinkage. Besides, intracellular NOS (NO synthase) inhibition and NO donation revealed the pro-apoptotic roles of NO in osteocytes. L-NAME (NOS inhibitor)-treated cells displayed no significant shrinkage under a larger force, whereas SNP (NO donor)-treated cells showed cell shrinkage and Annexin V fluorescence, indicating apoptosis. Collectively, our study demonstrates that larger force leads to NO production-mediated osteocyte shrinkage, implying an initial apoptotic response and highlighting the importance of NO production in bone damage.

1. Introduction

Bone continuously accumulates damage (Vashishth et al., 2000) due to mechanical load that eventually leads to bone fractures (Yeni and Fyhrie, 2002); thus, damaged bone is repaired to maintain its structural integrity. Bone damage is repaired by osteoclastic bone resorption followed by osteoblastic bone formation (Cardoso et al., 2009). Studies have shown that osteocyte apoptosis promotes bone resorption in mechanically overloaded bone regions (Kogianni et al., 2008; Verborgt et al., 2000). Microscopic observations have indicated numerous apoptotic osteocytes around micro-cracks and resorbed regions in mechanically overloaded bone (Verborgt et al., 2000), whereas apoptotic osteocytes reportedly accelerate bone resorption facilitated by osteoclast differentiation on the bone surface (Kogianni et al., 2008). These findings imply that osteocyte apoptosis is pivotal to osteoclastic bone resorption during bone repair; however, the mechanisms underlying osteocyte apoptosis following mechanical overloading remain unclear.

In vitro studies have shown that osteocytes response to mechanical stimuli is mediated by intracellular signaling molecules, such as nitric oxide (NO) (Bacabac et al., 2008; KleinNulend et al., 1995; Vatsa et al., 2006) and calcium ions (Ca^{2+}) (Adachi et al., 2009a, 2009b; Thi et al., 2013). NO is synthesized from L-arginine and O_2 by nitric oxide synthase (NOS) (Knowles and Moncada, 1994) and induces apoptosis in various cell types, including macrophages (Albina et al., 1993), neurons (Simmons and Murphy, 1992) and chondrocytes (Blanco et al., 1995). In several cell types (Kanaoka et al., 2000; Mancini et al., 2000; Shen et al., 1998; Yoshioka et al., 2003), the pro-apoptotic effects of NO occur at high concentrations, whereas anti-apoptotic effects at low concentrations. Thus, higher intracellular NO concentration

* Corresponding author at: 53 Shogoin-Kawahara-cho, Sakyo, Kyoto 606-8507, Japan.
E-mail address: adachi@infront.kyoto-u.ac.jp (T. Adachi).

https://doi.org/10.1016/j.jbiomech.2021.110245
0021-9290/

by mechanical stimulation could be a notable factor for osteocyte apoptosis. Although, under fluid flow shear stress, endothelial cells (Dimmeler et al., 1999) and chondrocytes (Lee et al., 2003) exhibit NO-mediated anti- and pro-apoptotic effects, respectively, the relationship between mechanical stimuli, NO, and apoptotic responses in osteocytes is unclear as these cells are located in unique mechanical environment. In lacunar-canalicular space (LCS) of bone, osteocytes attach to the bone matrix at locally located focal points, where mechanical stimuli affect cells via integrin under interstitial fluid flow in the LCS (Wang et al., 2007).

Magnetic tweezer mimics the *in vivo* mechanical environment surrounding osteocytes by locally applying mechanical stimuli to cells via magnetic beads attached to the cell surface, such as, focal adhesion translocation (Mack et al., 2004) and chromatin stretching (Tajik et al., 2016). In previous single-cell experiments, magnetic tweezer has been used to probe the effects of different stimuli on microscopically visualized cellular responses. Similarly, this study utilizes confocal microscopy combined with a magnetic tweezer and fibronectin-coated magnetic beads targeting cell surface integrin, to locally apply variable magnitude of force to osteocytes, detect apoptosis, and observe intracellular NO.

Herein, we elucidate the mechanism of apoptosis in mechanically overloaded osteocytes, focusing on the pro-apoptotic roles of NO. Osteocytes isolated from DMP1-EGFP mice were subjected to quantitative local mechanical stimuli using a magnetic tweezer. Cells were observed to examine the effects of force magnitude on apoptotic responses, especially focusing on cell shrinkage, represented by cell area decrease in several types of apoptotic cells (Kim et al., 2004; Porcelli et al., 2004; Tian et al., 2016). Furthermore, the cells were monitored to investigate the effects of force magnitude on intracellular NO production, whereas intracellular NOS inhibition indicated NO production necessary for mechanically stimulated apoptosis, and NO donation revealed the pro-apoptotic roles of NO in osteocytes.

2. Material and methods

2.1. Fibronectin-coated culture dishes

For osteocytes adhering to glass culture dishes (MatTek, Ashland, Massachusetts), their surface was modified with fibronectin, targeting integrin αvβ3 (Adair et al., 2005), which is dominantly expressed on osteocytes (Cabahug-zuckerman et al., 2018). The surface was treated with the linker molecule 0.2% poly-D-lysine (Sigma, Saint Louis, Missouri) at 37℃ for 1 h, rinsed with sterilized water, and modified with 0.2% fibronectin (Millipore, Burlington, Massachusetts) at 37℃ for 1 h. The plates were then rinsed with sterilized water and maintained dry until cell seeding.

2.2. Osteocyte isolation and primary culture

Osteocytes were isolated as described previously (Nakashima et al., 2011) from DMP1-EGFP mice (CAG-CAT-EGFP/Dmp1-*Cre* double-transgenic C57BL/6JJmsSlc) that express EGFP only when expressing the osteocyte-specific protein DMP1 (Toyosawa et al., 2001). Briefly, calvariae were extracted from 7 to 10-day-old mice, dissected, and collagen dissolved using collagenase solution (0.1% collagenase (Wako, Japan) and 0.2% Dispase Ⅱ (Godo Shusei, Japan) in BIB) at 37℃ for 20 min. The solution was removed by rinsing with PBS, and the mineralized bone tissue was decalcified using 5 mM EDTA (Dojindo, Japan) at 37℃ for 15 min. After further PBS rinsing to remove EDTA, the calvaria fragments were treated again with collagenase solution and EDTA in the same manner. Following the second and third collagenase treatments, the mixture was centrifuged at 500 rcf for 3 min, and the supernatant was added to the culture medium (α-MEM (Gibco, Waltham, MA) supplemented with 10% FBS (Gibco) and 1% antibiotics). Osteocytes were collected by repeated centrifugation, sparsely seeded on fibronectin-coated glass dishes at densities of 9.9×10^4 to 4.5×10^5 cells/cm^2, and cultured at 37℃ under 5% CO_2 for 2 h. Mice experiments were approved by the Animal Experimentation Committee (#Z-19–2-2) and Safety Committee for Recombinant DNA Experiments (#200004) of Kyoto University.

2.3. Fluorescence staining of F-actin in bone cells

To examine cellular morphology, F-actin was visualized by fluorescence staining. Briefly, the cells were fixed with 4% paraformaldehyde (Sigma, Saint Louis, Missouri) for 60 min, rinsed with PBS, incubated with Alexa Fluor 546 Phalloidin (Invitrogen, Carlsbad, California) for 60 min, and then rinsed with PBS.

2.4. Detection of osteocyte apoptosis

Cell shrinkage (Kim et al., 2004; Porcelli et al., 2004; Tian et al., 2016) is an initial apoptotic response. To detect osteocyte shrinkage, the changes in cell area $A(t)$ (μm^2, where t (s) indicates the time from the start of mechanical stimulation) defined as the EGFP-positive area were microscopically monitored, and then quantitatively assessed, as described in section 2.11. Additionally, plasma membrane degeneration, which is another apoptotic event, was visualized using Alexa Fluor 488 conjugated Annexin V (Tait et al., 1989) (Invitrogen) during early-apoptosis. Apoptotic cells were stained by incubation with Annexin V solution (2% Annexin V and 1.5 mM $CaCl_2$ in culture medium) at 37℃ under 5% CO_2 for 30 min and indicated much higher fluorescence intensity than GFP.

2.5. Fluorescence staining of intracellular NO in osteocytes

Intracellular NO in osteocytes was visualized using DAR-4 M AM (Goryo Chemical, Japan), which remains in the cytoplasm with hydrolyzed AM groups and exclusively emits fluorescence when bound to NO (Kojima et al., 2001). After exposure to DAR-4 M AM solution (1.25×10^{-3}% DAR-4 M AM in culture medium, including 0.01% Pluronic F-127 and 5.00×10^{-3}% Cremophor EL for cell membrane permeability) at 37℃ under 5% CO_2 for 30 min, the cells were incubated in fresh culture medium for 30 min to promote AM group hydrolyzation.

2.6. Inhibition of NO production in osteocytes

To examine the effects of NO on osteocyte apoptosis under mechanical stimulation, intracellular NOS was inhibited using L-NAME (Tan et al., 2007) (Dojindo, Japan). The cells were seeded with L-NAME at a final concentration of 1 mM, which was maintained constant during the experiments by supplementing additional L-NAME.

2.7. Introducing NO into osteocytes

To directly examine the effects of NO on osteocyte apoptosis, NO donation was conducted with SNP (Chen et al., 2005) (Sodium nitrosylpentacyanoferrate (III) dehydrate; Nacalai Tesque, Japan). First, osteocytes were isolated from the calvariae of 8–10-day-old C57BL/6JJmsSlc mice (Shimizu Laboratory Supplies, Japan) and cultured, as described in section 2.2. Second, ten Annexin V-negative osteocytes with slender cell processes were microscopically selected. Osteocytes were then treated with SNP at a final concentration of 50 mM at 37℃ under 5% CO_2 for 2 h. An observation interval longer than that in mechanical experiments was set to ensure to detect Annexin V fluorescence. Subsequent microscopic

observation detected Annexin V fluorescence in the selected osteocytes. Experiments were repeated five times. Each SNP experiment was independently performed on five different days, and the ten osteocytes tested for each experiment were selected from the same dish.

2.8. Magnetic tweezer and beads

Mechanical stimuli were applied to osteocytes using a magnetic tweezer (MagTw10-1200; RF Innovation, Japan; Fig. 1A; left) consisting of a PC permalloy (Ni 78%) round bar coiled with 1200 turns (100 turns per layer) of copper wire. The cone-shaped bar tip was polished at 45° from the central axis of the bar (Fig. 1A; right).

Magnetic beads (4.5 μm diameter; Dynabeads MyOne Tosylactivated, Invitrogen) were modified with fibronectin for adhering to osteocytes. Briefly, the beads were rinsed with PBS and incubated with fibronectin solution (200 μg/mL fibronectin and 0.1% BSA in sodium borate buffer) at 37℃ for 24 h for covalent binding of their tosyl groups to fibronectin. After removing the solution, the beads were treated with EDTA solution (2 mM EDTA and 0.1% BSA in PBS) at 5℃ for 5 min and incubated in 0.2 M Tris with 0.1% BSA at 37℃ for 4 h to inactivate the remaining tosyl groups.

2.9. Osteocyte mechanical stimulation using a magnetic tweezer

For osteocyte mechanical stimulation, the dishes were placed in a stage incubator (STG-IX3W and WSKMX-A17F, Tokai Hit, Japan) on the stage of a confocal laser scanning microscopy (FV-3000; Olympus, Japan; Fig. 1B). A three-degree-of-freedom micro manipulator (QP-3LH; Micro Support, Japan) was fixed at the central angle of the magnetic tweezer at 45° from the dish, and the tweezer tip was placed near EGFP-positive cells with a single bead. The tweezer applied mechanical stimuli to cells at a magnitude of 500 or 1000 pN that can experientially cause a difference in NO production, while 10 μm, which is higher than cell height, above the base of the dish to prevent any contacts (Fig. 1C). To correctly apply the set forces to the cells, the manipulator set the tweezer tip-bead distance at d (μm), as determined using force-distance (F-d) calibration curves (Fig. 1D; left). The electric currents driving the tweezer were set using a square-shaped wave with an amplitude of 0.1 or 0.3 A, frequency of 1 Hz, and duration of 600 s (0 s ≤ time t (s) ≤ 600 s; Fig. 1C). Each osteocyte of three controls (1000 pN force, 500 PN force, and 1000 pN + L-NAME) was tested on different days.

2.10. Calibration of F-d relationship

To calibrate the F-d relationship, magnetic beads were diffused into standard liquid for calibrating viscometers (JIS14000 Lot No.135; Nippon Grease, Japan) in glass dishes maintained at 37℃ by the stage incubator. Using a micro manipulator, the tweezer tip was placed in the liquid, and forces were applied to the beads using an electromagnetic force application device (MagF-Prototype; RF Innovation, Japan) with a square-wave electric current set at 0.01 Hz and a duty rate of 99%. Bead movements were monitored microscopically.

Images were analyzed using ImageJ (NIH) to evaluate the relationship between the force applied to the beads and tweezer tip-bead distance d (μm) based on bead movement (Fig. 1D; right). Bead velocity v (μm/s; $\Delta d/\Delta t$) was measured as barycentric coordinate displacement following the binarization of bead images. The force F (pN) applied to the beads was calculated using Stokes' equation:

$$F(v) = 6\pi\eta r v, \tag{1}$$

where, η (kg/μms) and r (μm) represent liquid viscosity and bead radius, respectively. Force F (pN) is expressed as follows:

$$F(d, I) = F_0 \times \left(\frac{d}{d_0}\right)^{C(I)}, \tag{2}$$

where, F_0 (pN), d_0 (μm), and I (A) (0.1 or 0.3 A) represent the force constant, distance constant, and electric current amplitude, respectively. Under constant I, the least square method determined estimated F-d curves using the measured F and d (Fig. 1D; left).

2.11. Osteocyte observation and image analysis

In mechanical stimulation experiments, confocal laser scanning microscopy was used to observe time-course changes in EGFP, DAR-4 M, and Annexin V fluorescence intensity in osteocytes with an exposure time of 200–500 ms at 1 s intervals for 3660 s (-60 s ≤ t ≤ 3600 s). Microscopic observation with transmitted light was conducted simultaneously. Fluorescence images were analyzed using ImageJ, with cell area $A(t)$ (μm^2) and ROIs for DAR-4 M analysis defined as the EGFP-positive area at time t. Within the ROIs, DAR-4 M fluorescence intensity was measured, averaged by the cell area $A(t)$, and normalized by its value at t = -60 s. Another image processing step prevented fluorescent variation in DAR-4 M images due to cell state and/or staining conditions. Total fluorescence intensity within each cell image was set as 600 at t = -60 s and, at t s, multiplied by the original rate of the total intensity at t s compared with that at -60 s.

In SNP experiments, cell body outlines, except for narrow processes and blebs, were traced in transmitted light images manually using ImageJ, and then cell area A (μm^2) was measured. To exclude the effects of arbitrary drawing on cell area tendency, an author without knowing SNP addition determined the lines in a random cell order. Thereafter, cell area averaged per single cell was calculated to compare between 0 and 2 h after SNP addition or only culture.

2.12. Statistical analysis

Paired t-tests were used to determine significant changes in normalized fluorescence intensity and cell area $A(t)$ as temporally averaged values before (-60 s ≤ t ≤ 0 s) and after (600 s ≤ t ≤ 660 s) mechanical stimulation. Student's t-tests were conducted to determine significant changes in the averaged cell area at 0 and 2 h after SNP addition or only culture, and the number of Annexin V-positive cells with and without SNP.

3. Results

3.1. Osteocyte isolation

To confirm successful osteocyte isolation from DMP1-EGFP mice, fluorescence imaging was performed to reveal the relationship between intracellular EGFP expression and osteocyte-specific morphology in the bone cells. In EGFP-positive cells (Fig. 2; upper left), fluorescence-labeled F-actin (Fig. 2; lower left) visualized several narrow cell processes elongating radially from the cell body, consistent with reported osteocyte-specific morphological characteristics (Hasegawa et al., 2018). Conversely, the labeled-F-actin in EGFP-negative cells (Fig. 2; upper right) revealed a cell morphology without slender cell processes (Fig. 2; lower right), indicating that these cells were not osteocytes. These findings demonstrated that EGFP-labeled osteocytes were successfully isolated from the mice.

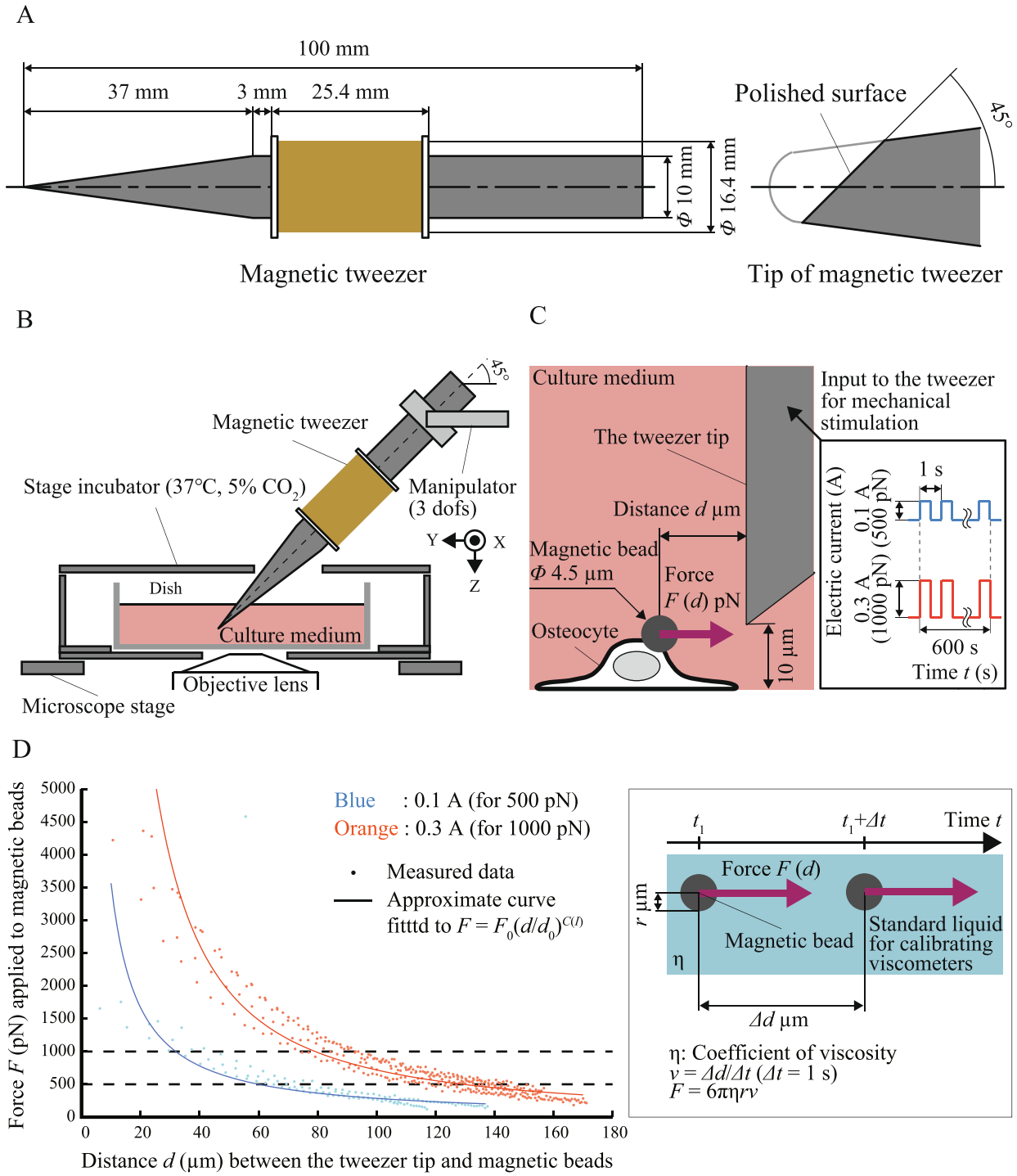

Fig. 1. Schematic representation of mechanical stimulation in osteocytes using a magnetic tweezer. (A) Magnetic tweezer (left), whose tip surface (right) was polished at an angle of 45° from the central axis (dashed-dotted lines). (B) Installation of the magnetic tweezer on a microscope stage with a manipulator controlling the position of the tweezer tip in culture dishes in the stage incubator. (C) Mechanical stimulation of osteocytes using the tweezer. Through the input of electric currents (right), the tweezer applied mechanical stimuli of force F = 500 or 1000 pN to the cells via magnetic beads at distance d (μm) between the magnetic bead and tweezer tip. (D) Calibration of F-d relationship. Force F (pN) was calculated using Stokes' equation $F = 6\pi\eta r v$ (right), and the distance d was measured. The relationship was fitted to $F = F_0(d/d_0)^{C(I)}$ (F_0, d_0, $C(I)$: constant). Blue and orange indicate electric current of 0.1 A (for 500 pN force) and 0.3 A (for 1000 pN force), respectively. Data dots and solid lines indicate measured data and approximate curves, respectively. (For interpretation of the references to colour in this figure legend, the reader is referred to the web version of this article.)

3.2. Osteocyte shrinkage by a larger force

Mechanical stimulations were performed to clarify the effects of force magnitude on osteocyte apoptosis. A magnetic tweezer applied a force of 500 or 1000 pN to osteocytes at 1 Hz for 600 s. To detect apoptosis, changes in cell area were observed over time t (stimulation: $0 \leq t \leq 600$ s). Mechanical stimulation at 500 pN did not cause cell shrinkage, as indicated by time-course cell observation (Fig. 3A EGFP and DIC) and the quantitative analysis (paired t-test; Fig. 3B) of cell area A (μm^2; i.e. EGFP-positive area) before and after stimulation. However, cell area gradually decreased after ($t \geq 600$ s) stimulation at 1000 pN (Fig. 3E EGFP and DIC), with sig-

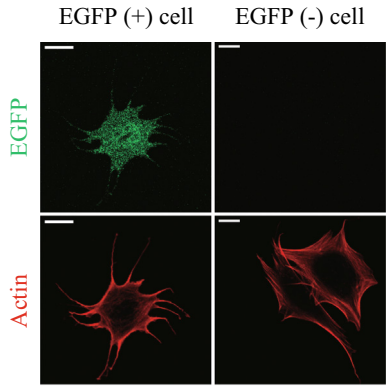

Fig. 2. Fluorescence images of bone cells derived from DMP1-EGFP mice calvariae. Left and right images indicate EGFP-positive (EGFP (+)) and -negative (EGFP (-)) cells, respectively. The upper and lower images show the intracellular fluorescence of EGFP and actin filaments, respectively. Scale bars 10 μm.

nificant shrinkage in cell area A (paired t-test, $p < 0.05$; Fig. 3F). Together, these findings showed that greater mechanical stimulation results in the shrinkage of osteocytes.

3.3. NO production in osteocytes by a larger force

Confocal microscopy was used to investigate the behavior of intracellular NO in mechanically stimulated osteocytes, with the NO indicator DAR-4 M. Mechanical stimulation at 500 pN did not induce NO production (Fig. 3A; DAR-4 M); however, DAR-4 M fluorescence intensity rapidly increased during (0 s $\leq t \leq$ 600 s) and after (600 s $\leq t \leq$ 1000 s) stimulation at 1000 pN in most cells (Fig. 3E; DAR-4 M). Besides, the quantitative analysis results indicated that the normalized fluorescence intensity (fluorescence intensity divided by cell area A (t) and intensity at t = -60 s) did not increase with 500 pN stimulation, except for a slight increase in DAR-4 M intensity at later stages within some cells, (Fig. 3C), whereas it drastically increased during and after stimulation at 1000 pN (Fig. 3G). DAR-4 M behaviors were validated by statistical comparison between normalized fluorescence intensity before and after stimulation (paired t-test; Fig. 3D and H). Thus, these data showed that larger force results in NO production in osteocytes.

3.4. Effects of NO production on osteocyte apoptosis

To investigate the roles of NO in mechanically stimulated apoptotic osteocytes, cells were subjected to NOS inhibition using L-NAME. After mechanical stimulation at 1000 pN, L-NAME-treated osteocytes did not produce NO, as indicated by DAR-4 M imaging and analysis (Fig. 4A; DAR-4 M, Fig. 4C and D), and displayed no significant cell shrinkage, as indicated by time-lapse observation (Fig. 4A; EGFP and DIC) and quantitative analyses of cell area (Fig. 4B). These data support that larger force causes intracellular NO production-mediated shrinkage of osteocytes.

To directly test whether NO induces osteocyte apoptosis, apoptosis was investigated in SNP (NO donor)-treated osteocytes. The majority of cells cultured without SNP for 2 h (SNP (-) cells) displayed no cell shrinkage or Annexin V fluorescence, which is an apoptosis marker (Fig. 4E-G; SNP (-)). However, significantly more cells cultured with SNP for 2 h (SNP (+) cells) displayed both cell shrinkage and Annexin V fluorescence (Fig. 4E-G; SNP (+), F; student's t-test, $p < 0.001$, G; student's t-test, $p < 0.05$). These findings confirm the pro-apoptotic roles of intracellular NO.

These findings demonstrate that larger force causes osteocyte shrinkage, suggesting an initial apoptotic response, via intracellular NO production.

4. Discussion

In this study, the quantitative local mechanical stimulation to osteocytes using a magnetic tweezer revealed that larger force induces intracellular NO production followed by an initial apoptotic sign i.e. cell shrinkage. Moreover, NOS inhibition and NO donation were performed to examine the pro-apoptotic roles of NO in osteocytes. To the best of our knowledge, our study is the first to imply an initial apoptotic response in osteocytes stimulated by large magnitude of force, mediated by intracellular NO production.

Previous studies have reported osteocyte apoptosis around both the bone surface and resorption areas in mechanically overloaded bones (Verborgt et al., 2000) and that apoptotic osteocytes promote osteoclastic differentiation (Kogianni et al., 2008). Although these studies indicate that mechanically overloaded apoptotic osteocytes are vital for bone resorption, few reports have focused on the apoptosis mechanism of mechanically overloaded osteocytes. Previous experiments using isolated osteocytes have demonstrated that cell apoptosis is triggered by substrate deformation via ERK activation, which is involved in cell growth (Hoshi et al., 2014); however, ERK reportedly suppresses apoptosis in osteocyte-like cells under substrate deformation (Plotkin et al., 2005). As ERK is activated by NO (Kim et al., 2002), rapid NO production may affect osteocyte apoptosis mediated by excessive ERK activation. Nevertheless, the effects of NO on apoptosis in mechanically overloaded osteocytes are poorly understood, and this study is the first to investigate such effects.

Osteocytes are subjected to mechanical stimuli due to bone matrix deformation (Adachi et al., 2009a) and interstitial fluid flow in the lacunar-canalicular system (Thi et al., 2013), which are thought to be transmitted intracellularly (Thi et al., 2013; You et al., 2004) via plasma membrane proteins, such as integrin (Cabahug-zuckerman et al., 2018) and piezo1 (Sasaki et al., 2020). Here, we used a magnetic tweezer to locally apply mechanical stimuli to membrane proteins via micro beads adhering to the cell surface.

NO production requires NOS (Knowles and Moncada, 1994), which has three different isozymes: nNOS, eNOS and, iNOS (Marletta, 1993). nNOS (Bredt and Snyder, 1990) and eNOS (Forstermann et al., 1991) are activated in the presence of intracellular Ca^{2+}, which increases in mechanically stimulated osteocytes (Adachi et al., 2009a, 2009b; Thi et al., 2013), likely inducing NO production as observed in this study. Several types of Ca^{2+} channels are co-expressed with integrin in osteocytes (Cabahug-zuckerman

Fig. 3. Apoptosis and NO production in mechanically stimulated osteocytes. The magnetic tweezer applied mechanical stimuli of F = 500 pN (A-D) or 1000 pN (E-H) to osteocytes. (A)(E) Microscopic imaging of cell area and intracellular NO. Mechanical stimuli (0 $\leq$ time t (s) $\leq$ 600 s) were applied to the cells after a no-stimulation period (-60 s $\leq t \leq$ 0 s). EGFP (upper) and DIC (middle) images showing time-course changes in the cell area. DAR-4 M fluorescence images (lower) indicating the behavior of intracellular NO. Yellow lines are cell outlines. Scale bars 10 μm. (B)(F) Effects of force F on cell area A. Paired t-tests determined significant changes in cell area A (μm^2) evaluated as temporally averaged values before (-60 s $\leq t \leq$ 0 s) and after (600 s $\leq t \leq$ 660 s) mechanical stimulation ($^*p < 0.05$). (C)(G) Time-course changes in DAR-4 M−normalized fluorescence intensity with enlarged views (0 $\leq t \leq$ 700 s). Vertical left and right dashed lines indicate the start and end of mechanical stimulation, respectively. (D)(H) Effects of force F on normalized fluorescence intensity. Paired t-tests determined significant change in normalized fluorescence intensity evaluated as temporally averaged values before (-60 s $\leq t \leq$ 0 s) and after (600 s $\leq t \leq$ 660 s) mechanical stimulation ($^*p < 0.05$).

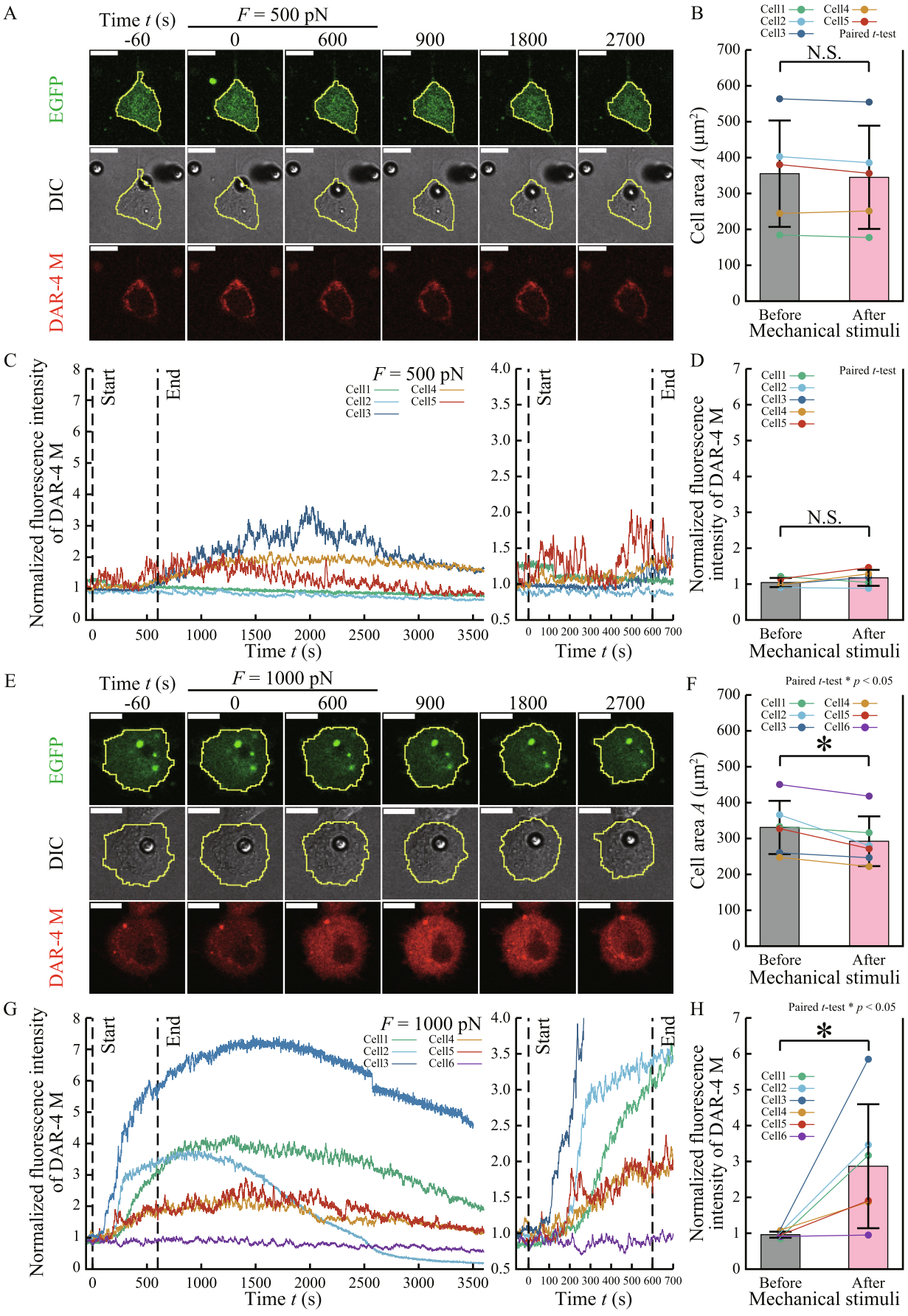
A
Time t (s)
F = 500 pN
-60
0
600
900
1800
2700
EGFP
DIC
DAR-4 M
B
Cell1
Cell2
Cell3
Cell4
Cell5
Paired t-test
N.S.
Cell area A (μm²)
Before
After
Mechanical stimuli
C
Start
End
F = 500 pN
Normalized fluorescence intensity of DAR-4 M
Time t (s)
D
Paired t-test
N.S.
Normalized fluorescence intensity of DAR-4 M
Before
After
Mechanical stimuli
E
Time t (s)
F = 1000 pN
-60
0
600
900
1800
2700
EGFP
DIC
DAR-4 M
F
Paired t-test * p < 0.05
Cell1
Cell2
Cell3
Cell4
Cell5
Cell6
*
Cell area A (μm²)
Before
After
Mechanical stimuli
G
Start
End
F = 1000 pN
Normalized fluorescence intensity of DAR-4 M
Time t (s)
H
Paired t-test * p < 0.05
*
Normalized fluorescence intensity of DAR-4 M
Before
After
Mechanical stimuli

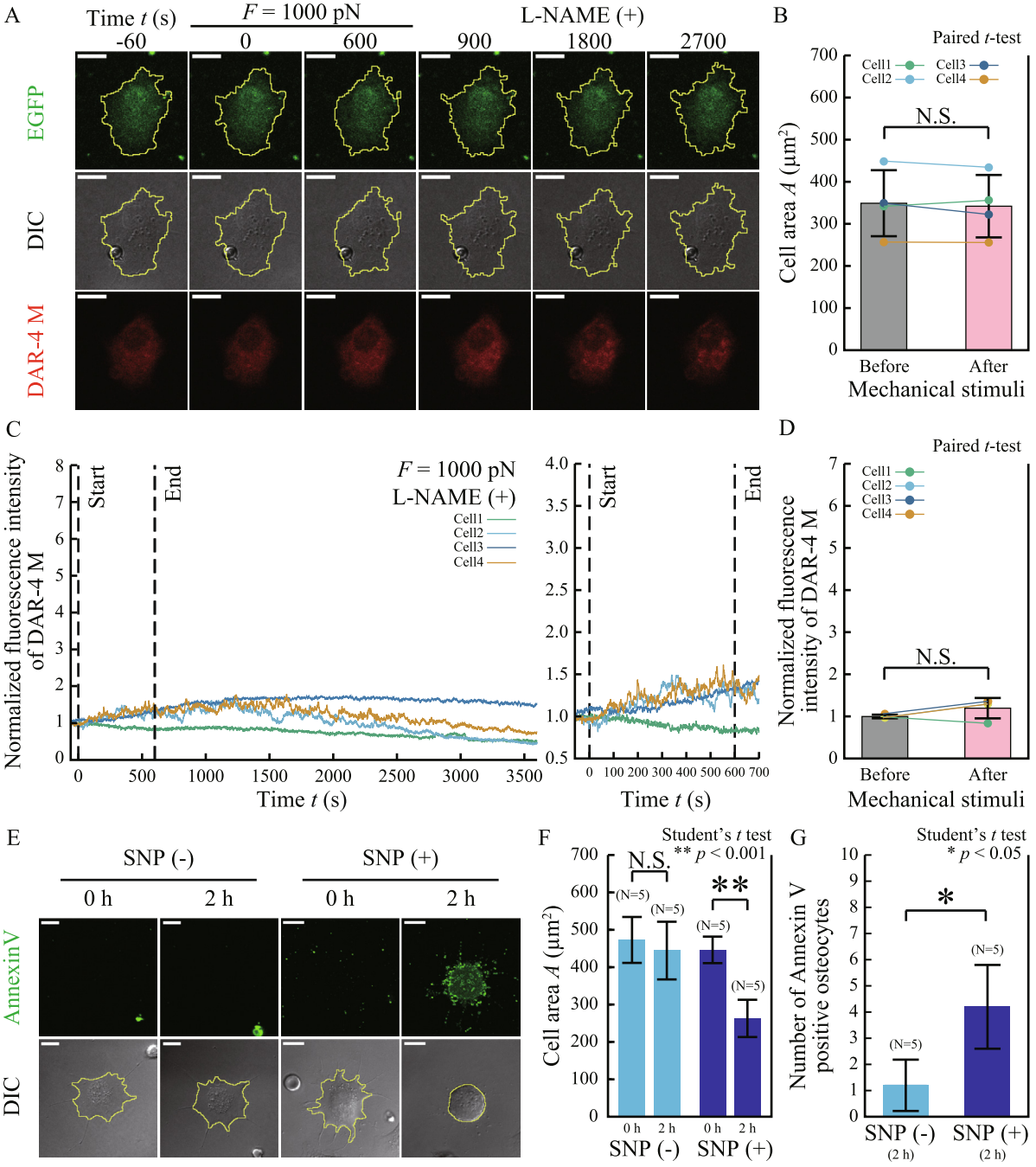

Fig. 4. Effects of NO on apoptosis in mechanically stimulated osteocytes. (A) Effects of NOS inhibition on mechanically stimulated osteocytes. As a negative control, the magnetic tweezer applied 1000 pN force to L-NAME (NOS inhibitor)-treated osteocytes. EGFP (upper) and DIC (middle) images showing the time-course changes in the cell area. DAR-4 M fluorescence images (lower) indicating the behavior of intracellular NO. (B) Effects of force F on cell area. A paired t-test determined significant changes in cell area A (μm^2) evaluated as temporally averaged values before ($-60\ s \le t \le 0\ s$) and after ($600\ s \le t \le 660\ s$) mechanical stimulation. (C) Time-course changes in DAR-4 M normalized fluorescence intensity with enlarged views ($0 \le t \le 700$ s). Vertical left and right dashed lines indicate the start and end of mechanical stimulation, respectively. (D) Effects of force F on normalized fluorescence intensity. A paired t-test determined significant changes in normalized fluorescence intensity evaluated as temporally averaged values before ($-60\ s \le t \le 0\ s$) and after ($600\ s \le t \le 660\ s$) mechanical stimulation. (E-G) Effects of NO donation on osteocyte apoptosis. As a positive control, Annexin V fluorescence was examined in osteocytes with or without 2 h of exposure to a NO donor (SNP). (E) Microscopic observation showing Annexin V fluorescence and cell shrinkage in SNP-treated cells. (F, G) Student's t-tests determined significant change in (F) cell area A (μm^2) during 2 h treatment, and (G) the number of Annexin V-positive cells between SNP (-) and (+) cells ($^*p < 0.05$, $^{**}p < 0.001$). A single SNP experiment tested ten cells. For reproducibility, independent experiments were repeated five times. Yellow lines indicate cell outlines. Scale bars 10 μm.

et al., 2018); therefore, the influx of extracellular Ca^{2+} may result from the mechanical opening of Ca^{2+} channels via membrane proteins, such as integrin. Moreover, fluid flow stress experiments have demonstrated an increase in both intracellular Ca^{2+} concentration and NO production in osteocyte-like cells (Bakker et al., 2009). However, the relationships between mechanical overload, Ca^{2+} influx, and NO production in osteocytes remain unclear.

Unlike nNOs and eNOS, iNOS-mediated NO production is induced in a Ca^{2+}-independent manner (Stuehr et al., 1991) and is triggered by biochemical stimuli such as cytokines, in neurons (Chiou et al., 2000) and myocytes (Balligand et al., 1994). Similar to neurons (Chiou et al., 2000), mechanically overloaded osteocytes may undergo iNOS-mediated apoptosis; however, our experiments did not show drastic NO production induced by a rapid increase in

underexpressed intracellular iNOS (Balligand et al., 1994; Chiou et al., 2000). Therefore, further studies are required to identify NOS isozymes that are involved in the process.

In our study, 1000 pN force resulted in a rapid increase in intracellular NO concentration in osteocytes, followed by cell shrinkage. Increased NO concentration affects the activities of cell death-related biomolecules; in fact, the state and effects of various intracellular proteins are dependent on intracellular NO concentration (Ridnour et al., 2005; Thomas et al., 2008, 2004). For instance, in breast cancer cells, ERK and apoptosis-inducing factors such as HIF-1α and p53 are reportedly activated and stabilized under specific concentrations of NO, respectively (Thomas et al., 2004). Similarly, the angiogenesis-inhibiting factor TSP1 is expressed in a NO concentration-dependent manner in endothelial cells (Ridnour et al., 2005). Moreover, NO concentration may affect cell fate by promoting and suppressing endothelial cell apoptosis at high and low concentrations, respectively (Shen et al., 1998). Similarly, macrophages undergo apoptotic chromatin condensation under high NO concentration, whereas they survive under low concentration (Yoshioka et al., 2003). Regarding bone cells, a previous study reported that a high NO donor concentration induced apoptosis-specific DNA fragmentation in osteoblasts, whereas low NO donor concentration induced osteoblast growth but caused no DNA fragmentation (Mancini et al., 2000). Similarly, apoptosis of osteoclasts occurred under high NO concentration, but not under low concentration (Kanaoka et al., 2000). The previously reported anti-apoptotic effects of NO in osteocytes (Hasegawa et al., 2018) may have occurred under low NO concentrations induced by small forces such as 500 pN in this study. Therefore, the reported effects of NO concentration on cell fate could explain osteocyte apoptosis mediated by intracellular drastic NO production.

Mechanical stimulation with a 1000 pN force did not evoke Annexin V fluorescence in all but one osteocyte which emitted fluorescence following cell shrinkage (Fig. A1). Longer cell observation might enable to detect Annexin V fluorescence in force experiments as cell membrane regeneration detected by Annexin V could clearly occur after hours of apoptosis induction (Demchenko, 2013). Similarly, blebbing observed in SNP experiments was rarely detected in force experiments. As osteocyte blebbing could occur after cell shrinkage in apoptotic process as reported in melanoma cells (Andrade et al., 2010) and neurons (Tanaka et al., 2015), SNP-induced blebbing might occur as a later apoptotic event due to longer observation time or higher NO concentration than that in force experiments.

This study did not quantitatively compare intracellular NO levels between two distinct conditions, namely mechanical stimulation and NO addition; therefore, NO concentrations in largely mechano-stimulated osteocytes may not be as high as that in NO-donated osteocytes and may be insufficient to induce apoptosis. The effects of intracellular NO concentration on apoptosis (discussed above) do not allow to quantitatively compare SNP data with mechanical stimulation data. However, SNP experiments showed pro-apoptotic effects of intracellular NO in osteocytes, and L-NAME data (Fig. 4A-D) indicated intracellular NO production required for cell shrinkage, implying that mechanically-stimulated intracellular NO production triggers osteocyte apoptosis. Further studies should confirm NO-induced osteocyte apoptosis by removing the effects of other NOS-mediated products such as L-citrulline. Future studies should elucidate how force magnitude determines NO production, which cell surface proteins stimulate NOS, and which molecules NO affects in the apoptotic signaling pathway.

5. Conclusion

Mechanical overload-induced apoptosis plays a pivot role in damaged bone resorption and repair. This study aimed to elucidate the mechanism underlying apoptosis in mechanically overloaded osteocytes, with a focus on the pro-apoptotic roles of intracellular NO. We found that large magnitude of force induces NO production-mediated osteocyte shrinkage, implying an initial apoptotic response. Thus, our study proposes that NO production is crucial for the remodeling of damaged bone.

Declaration of Competing Interest

The authors declare that they have no known competing financial interests or personal relationships that could have appeared to influence the work reported in this paper.

Acknowledgements

This work was partially supported by a Grant-in-Aid for JSPS fellows (18J23041) from JSPS and AMED-CREST (JP20gm0810003) from AMED, Japan.

Appendix

(See Fig. A1)

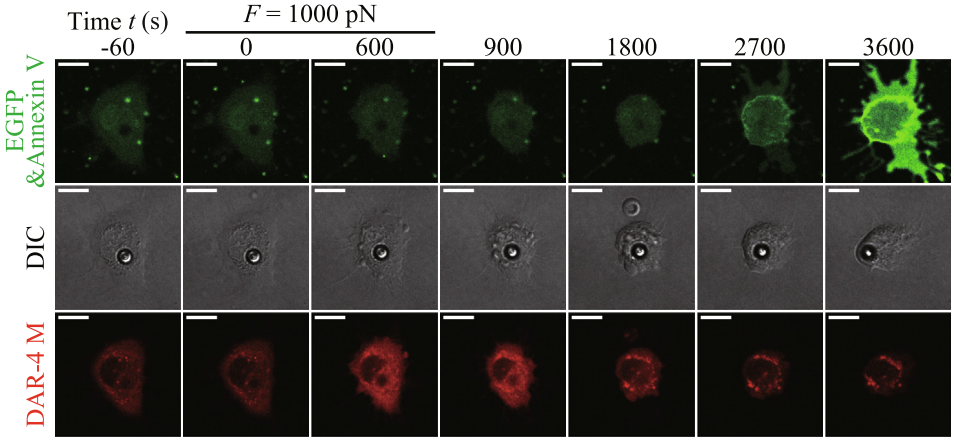

Fig. A1. Apoptosis and NO production in a single mechanically stimulated osteocyte. The magnetic tweezer applied a force of 1000 pN to the osteocyte. Time *t* (s) indicates time from the beginning of mechanical stimulation. DIC, DAR-4 M fluorescence, and Annexin V fluorescence images indicating cell shrinkage, intracellular NO production, and plasma membrane degeneration, respectively. Scale bars 10 μm.

References

Adachi, T., Aonuma, Y., Ito, S., Tanaka, M., Hojo, M., Takano-Yamamoto, T., Kamioka, H., 2009a. Osteocyte calcium signaling response to bone matrix deformation. J. Biomech. 42, 2507–2512. https://doi.org/10.1016/j.jbiomech.2009.07.006.

Adachi, T., Aonuma, Y., Tanaka, M., Hojo, M., Takano-Yamamoto, T., Kamioka, H., 2009b. Calcium response in single osteocytes to locally applied mechanical stimulus: Differences in cell process and cell body. J. Biomech. 42, 1989–1995. https://doi.org/10.1016/j.jbiomech.2009.04.034.

Adair, B.D., Xiong, J., Maddock, C., Goodman, S.L., Arnaout, M.A., Yeager, M., 2005. Three-dimensional EM structure of the ectodomain of integrin αVβ3 in a complex with fibronectin. J. Cell Biol. 168, 1109–1118. https://doi.org/10.1083/jcb.200410068.

Albina, J.E., Cui, S.J., Mateo, R.B., Reichner, J.S., 1993. Nitric oxide-mediated apoptosis in murine peritoneal macrophages. J. Immunol. 150, 5080–5085. https://doi.org/10.1016/0169-4758(93)90226-6.

Andrade, R., Crisol, L., Prado, R., Boyano, M.D., Arluzea, J., Arechaga, J., 2010. Plasma membrane and nuclear envelope integrity during the blebbing stage of apoptosis: a time-lapse study. Biol. Cell 102, 25–35. https://doi.org/10.1042/BC20090077.

Bacabac, R.G., Mizuno, D., Schmidt, C.F., Mackintosh, F.C., Van Loon, J.J.W.A., Klein-Nulend, J., Smit, T.H., 2008. Round versus flat : Bone cell morphology, elasticity, and mechanosensing. J. Biomech. 41, 1590–1598. https://doi.org/10.1016/j.jbiomech.2008.01.031.

Bakker, A.D., da Silva, V.C., Krishnan, R., Bacabac, R.G., Blaauboer, M.E., Lin, Y.C., Marcantonio, R.A.C., Cirelli, J.A., J, K.-N., 2009. Tumor Necrosis Factor α and Interleukin-1β Modulate Calcium and Nitric Oxide Signaling in Mechanically Stimulated Osteocytes. Arthritis Rheum. 60, 3336–3345. 10.1002/art.24920

Balligand, J.L., Ungureanu-Longrois, D., Simmons, W.W., Pimental, D., Malinski, T.A., Kapturczak, M., Taha, Z., Lowenstein, C.J., Davidoff, A.J., Kelly, R.A., Smith, T.W., Michel, T., 1994. Cytokine-inducible nitric oxide synthase (iNOS) expression in cardiac myocytes. Characterization and regulation of iNOS expression and detection of iNOS activity in single cardiac myocytes in vitro. J. Biol. Chem. 269, 27580–27588.

Blanco, F.J., Ochs, R.L., Schwarz, H., Lotz, M., 1995. Chondrocyte apoptosis induced by nitric oxide. Am. J. Pathol. 146, 75–85.

Bredt, D.S., Snyder, S.H., 1990. Isolation of nitric oxide synthetase, a calmodulin-requiring enzyme. Proc. Natl. Acad. Sci. U. S. A. 87, 682–685. https://doi.org/10.1073/pnas.87.2.682.

Cabahug-zuckerman, P., Jr, R.F.S., Majeska, R.J., Thi, M.M., Spray, D.C., Weinbaum, S., Schaffler, M.B., 2018. Potential Role for a Specialized b3 Integrin-Based Structure On Osteocyte Processes in Bone Mechanosensation. J. Orthop. Res. 36, 642–652. 10.1002/jor.23792

Cardoso, L., Herman, B.C., Verborgt, O., Laudier, D., Majeska, R.J., Schaffler, M.B., 2009. Osteocyte Apoptosis Controls Activation of Intracortical Resorption in Response to Bone Fatigue. J. Bone Miner. Res. 24, 597–605. https://doi.org/10.1359/jbmr.081210.

Chen, R.M., Chen, T.L., Chiu, W.T., Chang, C.C., 2005. Molecular mechanism of nitric oxide-induced osteoblast apoptosis. J. Orthop. Res. 23, 462–468. https://doi.org/10.1016/j.orthres.2004.08.011.

Chiou, W.-F., Chen, C.-F., Lin, J.-J., 2000. Mechanisms of suppression of inducible nitric oxide synthase (iNOS) expression in RAW 264.7 cells by andrographolide. Br. J. Pharmacol. 129, 1553–1560. https://doi.org/10.1038/sj.bjp.0703191.

Demchenko, A.P., 2013. Beyond annexin V: fluorescence response of cellular membranes to apoptosis. Cytotechnology 65, 157–172. https://doi.org/10.1007/s10616-012-9481-y.

Dimmeler, S., Hermann, C., Galle, J., Zeiher, A.M., 1999. Upregulation of Superoxide Dismutase and Nitric Oxide Synthase Mediates the Apoptosis-Suppressive Effects of Shear Stress on Endothelial Cells. Arterioscler. Thromb. Vasc. Biol. 19, 656–664. https://doi.org/10.1161/01.ATV.19.3.656.

Forstermann, U., Pollock, J.S., Schmidt, H.H.H.W., Heller, M., Murad, F., 1991. Calmodulin-dependent endothelium-derived relaxing factor/nitric oxide synthase activity is present in the particulate and cytosolic fractions of bovine aortic endothelial cells. Proc. Natl. Acad. Sci. U. S. A. 88, 1788–1792. https://doi.org/10.1073/pnas.88.5.1788.

Hasegawa, T., Yamamoto, T., Hongo, H., Qiu, Z., Abe, M., Kanesaki, T., Tanaka, K., Endo, T., de Freitas, P.H.L., Li, M.Q., Amizuka, N., 2018. Three-dimensional ultrastructure of osteocytes assessed by focused ion beam-scanning electron microscopy (FIB-SEM). Histochem. Cell Biol. 149, 423–432. https://doi.org/10.1007/s00418-018-1645-1.

Hoshi, K., Kawaki, H., Takahashi, I., Takeshita, N., Seiryu, M., Murshid, S.A., Masuda, T., Anada, T., Kato, R., Kitaura, H., Suzuki, O., Takano-Yamamoto, T., 2014. Compressive force-produced CCN2 induces osteocyte apoptosis through ERK1/2 pathway. J. Bone Miner. Res. 29, 1244–1257. https://doi.org/10.1002/jbmr.2115.

Kanaoka, K., Kobayashi, Y., Hashimoto, F., Nakashima, T., Shibata, M., Kobayashi, K., Kato, Y., Sakai, H., 2000. A Common Downstream Signaling Activity of Osteoclast Survival Factors That Prevent Nitric Oxide-Promoted osteoclast apoptosis. Endocrinology 141, 2995–3005. https://doi.org/10.1210/endo.141.8.7603.

Kim, S.-J., Ju, J.-W., Oh, C.-D., Yoon, Y.-M., Song, W.K., Kim, J.-H., Yoo, Y.J., Bang, O.-S., Kang, S.-S., Chun, J.-S., 2002. ERK-1/2 and p38 Kinase Oppositely Regulate Nitric Oxide-induced Apoptosis of Chondrocytes in Association with p53, Caspase-3, and Differentiation Status. J. Biol. Chem. 277, 1332–1339. https://doi.org/10.1074/jbc.M107231200.

Kim, T., Tchah, H., Cho, E.H., Kook, M.S., 2004. Evaluation for Safety of Cultured Corneal Fibroblasts with Cotreatment of Alcohol and Mitomycin C. Invest. Ophthalmol. Vis. Sci. 45, 86–92. https://doi.org/10.1167/iovs.03-0520.

KleinNu-lend, J., Semeins, C.M., Ajubi, N.E., Nijweide, P.J., Burger, E.H., 1995. Pulsating Fluid Flow Increases Nitric Oxide (NO) Synthesis by Osteocytes but Not Periosteal Fibroblasts - Correlation with Prostaglandin Upregulation. Biochem. Biophys. Res. Commun. 217, 640–648. https://doi.org/10.1006/bbrc.1995.2822.

Knowles, R.G., Moncada, S., 1994. Nitric oxide synthases in mammals. Biochem. J. 298, 249–258. https://doi.org/10.1042/bj2980249.

Kogianni, G., Mann, V., Noble, B.S., 2008. Apoptotic bodies convey activity capable of initiating osteoclastogenesis and localized bone destruction. J. Bone Miner. Res. 23, 915–927. https://doi.org/10.1359/JBMR.080207.

Kojima, H., Hirotani, M., Nakatsubo, N., Kikuchi, K., Urano, Y., Higuchi, T., Hirata, Y., Nagano, T., 2001. Bioimaging of Nitric Oxide with Fluorescent Indicators Based on the Rhodamine Chromophore. Anal. Chem. 73, 1967–1973. https://doi.org/10.1021/ac001136i.

Lee, M.S., Trindade, M.C.D., Ikenoue, T., Goodman, S.B., Schurman, D.J., Smith, R.L., 2003. Regulation of nitric oxide and bcl-2 expression by shear stress in human osteoarthritic chondrocytes in vitro. J. Cell. Biochem. 90, 80–86. https://doi.org/10.1002/jcb.10611.

Mack, P.J., Kaazempur-Mofrad, M.R., Karcher, H., Lee, R.T., Kamm, R.D., 2004. Force-induced focal adhesion translocation: Effects of force amplitude and frequency. Am. J. Physiol. - Cell Physiol. 287, C954–C962. https://doi.org/10.1152/ajpcell.00567.2003.

Mancini, L., Moradi-Bidhendi, N., Becherini, L., Martineti, V., MacIntyre, I., 2000. The Biphasic Effects of Nitric Oxide in Primary Rat Osteoblasts Are cGMP Dependent. Biochem. Biophys. Res. Commun. 274, 477–481. https://doi.org/10.1006/bbrc.2000.3164.

Marletta, M.A., 1993. Nitric Oxide Synthase Structure and Mechanism. J. Biol. Chem. 268, 12231–12234.

Nakashima, T., Hayashi, M., Fukunaga, T., Kurata, K., Oh-hora, M., Feng, J.Q., Bonewald, L.F., Kodama, T., Wutz, A., Wagner, E.F., Penninger, J.M., Takayanagi, H., 2011. Evidence for osteocyte regulation of bone homeostasis through RANKL expression. Nat. Med. 17, 1231–1234. https://doi.org/10.1038/nm.2452.

Plotkin, L.I., Mathov, I., Aguirre, J.I., Parfitt, A.M., Manolagas, S.C., Bellido, T., 2005. Mechanical stimulation prevents osteocyte apoptosis : requirement of integrins, Src kinases, and ERKs. Am. J. Physiol. Physiol. 289, C633–C643. https://doi.org/10.1152/ajpcell.00278.2004.

Porcelli, A.M., Ghelli, A., Zanna, C., Valente, P., Ferroni, S., Rugolo, M., 2004. Apoptosis induced by staurosporine in ECV304 cells requires cell shrinkage and upregulation of Cl- conductance. Cell death Differ. 11, 655–662. https://doi.org/10.1038/sj.cdd.4401396.

Ridnour, L.A., Isenberg, J.S., Espey, M.G., Thomas, D.D., Roberts, D.D., Wink, D.A., 2005. Nitric oxide regulates angiogenesis through a functional switch involving thrombospondin-1. Proc. Natl. Acad. Sci. U. S. A. 102, 13147–13152. https://doi.org/10.1073/pnas.0502979102.

Sasaki, F., Hayashi, M., Mouri, Y., Nakamura, S., Adachi, T., Nakashima, T., 2020. Mechanotransduction via the Piezo1-Akt pathway underlies Sost suppression in osteocytes. Biochem. Biophys. Res. Commun. 521, 806–813. https://doi.org/10.1016/j.bbrc.2019.10.174.

Shen, Y.H., Wang, X.L., Wilcken, D.E.L., 1998. Nitric oxide induces and inhibits apoptosis through different pathways. FEBS Lett. 433, 125–131. https://doi.org/10.1016/S0014-5793(98)00844-8.

Simmons, M.L., Murphy, S., 1992. Induction of Nitric Oxide Synthase in Glial Cells. J. Neurochem. 59, 897–905. https://doi.org/10.1111/j.1471-4159.1992.tb08328.x.

Stuehr, D.J., Cho, H.J., Kwon, N.S., Weise, M.F., Nathan, C.F., 1991. Purification and characterization of the cytokine-induced macrophage nitric oxide synthase : An FAD- and FMN-containing flavoprotein. Proc. Natl. Acad. Sci. U. S. A. 88, 7773–7777. https://doi.org/10.1073/pnas.88.17.7773.

Tait, J.F., Gibson, D., Fujikawa, K., 1989. Phospholipid Binding Properties of Human Placental Anticoagulant Protein-I, a Member of the Lipocortin Family. J. Biol. Chem. 264, 7944–7949.

Tajik, A., Zhang, Y.J., Wei, F.X., Sun, J., Jia, Q., Zhou, W.W., Singh, R., Khanna, N., Belmont, A.S., Wang, N., 2016. Transcription upregulation via force-induced direct stretching of chromatin. Nat. Mater. 15, 1287–1296. https://doi.org/10.1038/NMAT4729.

Tan, S.D., de Vries, T.J., Kuijpers-jagtman, A.M., Semeins, C.M., Everts, V., Klein-Nulend, J., 2007. Osteocytes subjected to fluid flow inhibit osteoclast formation and bone resorption. Bone 41, 745–751. https://doi.org/10.1016/j.bone.2007.07.019.

Tanaka, A., Tanaka, R., Kasai, N., Tsukada, S., Okajima, T., Sumitomo, K., 2015. Time-lapse imaging of morphological changes in a single neuron during the early stages of apoptosis using scanning ion conductance microscopy. J. Struct. Biol. 191, 32–38. https://doi.org/10.1016/j.jsb.2015.06.002.

Thi, M.M., Suadicani, S.O., Schaffler, M.B., Weinbaum, S., Spray, D.C., 2013. Mechanosensory responses of osteocytes to physiological forces occur along processes and not cell body and require αVβ3 integrin. Proc. Natl. Acad. Sci. U. S. A. 110, 21012–21017. https://doi.org/10.1073/pnas.1321210110.

Thomas, D.D., Espey, M.G., Ridnour, L.A., Hofseth, L.J., Mancardi, D., Harris, C.C., Wink, D.A., 2004. Hypoxic inducible factor 1α, extracellular signal-regulated kinase, and p53 are regulated by distinct threshold concentrations of nitric oxide. Proc. Natl. Acad. Sci. U. S. A. 101, 8894–8899. https://doi.org/10.1073/pnas.0400453101.

Thomas, D.D., Ridnour, L.A., Isenberg, J.S., Flores-santana, W., Switzer, C.H., Donzelli, S., Hussain, P., Vecoli, C., Paolocci, N., Ambs, S., Colton, C.A., Harris, C.C., Roberts,

D.D., Wink, D.A., 2004. The chemical biology of nitric oxide: Implications in cellular signaling. Free Radic. Bioligy Med. 45, 18–31. https://doi.org/10.1016/j.freeradbiomed.2008.03.020.

Tian, Q., Wu, S., Dai, Z., Yang, J., Zheng, J., Zheng, Q., Liu, Y., 2016. Iron overload induced death of osteoblasts in vitro: involvement of the mitochondrial apoptotic pathway. PeerJ 4,. https://doi.org/10.7717/peerj.2611 e2611.

Toyosawa, S., Shintani, S., Fujiwara, T., Ooshima, T., Sato, A., Ijuhin, N., Komori, T., 2001. Dentin Matrix Protein 1 Is Predominantly Expressed in Chicken and Rat Osteocytes But Not in Osteoblasts. J. Bone Miner. Res. 16, 2017–2026. https://doi.org/10.1359/jbmr.2001.16.11.2017.

Vashishth, D., Koontz, J., Qiu, S.J., Lundin-Cannon, D., Yeni, Y.N., Schaffler, M.B., Fyhrie, D.P., 2000. In Vivo Diffuse Damage in Human Vertebral Trabecular Bone. Bone 26, 147–152. https://doi.org/10.1016/S8756-3282(99)00253-7.

Vatsa, A., Mizuno, D., Smit, T.H., Schmidt, C.F., Mackintosh, F.C., Klein-Nulend, J., 2006. Bio imaging of intracellular NO production in single bone cells after mechanical stimulation. J. Bone Miner. Res. 21, 1722–1728. https://doi.org/10.1359/JBMR.060720.

Verborgt, O., Gibson, G.J., Schaffler, M.B., 2000. Loss of Osteocyte Integrity in Association with Microdamage and Bone Remodeling After Fatigue In Vivo. J. Bone Miner. Res. 15, 60–67. https://doi.org/10.1359/jbmr.2000.15.1.60.

Wang, Y., McNamara, L.M., Schaffler, M.B., Weinbaum, S., 2007. A model for the role of integrins in flow induced mechanotransduction in osteyocytes. Proc. Natl. Acad. Sci. U. S. A. 104, 15941–15946. https://doi.org/10.1073/pnas.0707246104.

Yeni, Y.N., Fyhrie, D.P., 2002. Fatigue Damage-Fracture Mechanics Interaction in Cortical Bone. Bone 30, 509–514. https://doi.org/10.1016/S8756-3282(01)00696-2.

Yoshioka, Y., Yamamuro, A., Maeda, S., 2003. Nitric oxide at a low concentration protects murine macrophage RAW264 cells against nitric oxide-induced death via cGMP signaling pathway. Br. J. Pharmacol. 139, 28–34. https://doi.org/10.1038/sj.bjp.0705206.

You, L., Weinbaum, S., Cowin, S.C., Schaffler, M.B., 2004. Ultrastructure of the Osteocyte Process and its Pericellular Matrix. Anat. Rec. Part A - Discov. Mol. Cell. Evol. Biol. 278A, 505–513. https://doi.org/10.1002/ar.a.20050.